HHS Public Access

Author manuscript

Stroke. Author manuscript; available in PMC 2017 July 01.

Published in final edited form as:

Stroke. 2016 July ; 47(7): 1782–1788. doi:10.1161/STROKEAHA.116.013320.

Added Value of Vessel Wall MR Imaging in the Differentiation of Moyamoya Vasculopathies in a Non-Asian Cohort

Mahmud Mossa-Basha, MD,
University of Washington, Department of Radiology, 1959 NE Pacific St, Box 357115, Seattle, WA 98195

Adam de Havenon, MD,
University of Utah, Department of Neurology, Salt Lake City, UT, USA

Kyra J. Becker, MD,
University of Washington, Department of Neurology, Seattle, WA, USA

Danial K. Hallam, MD,
University of Washington, Department of Radiology, Seattle, WA, USA

Michael R. Levitt, MD,
University of Washington, Department of Neurosurgery, Seattle, WA, USA

Wendy A. Cohen, MD,
University of Washington, Department of Radiology, Seattle, WA, USA

Daniel S. Hippe, MS,
University of Washington, Department of Radiology, Seattle, WA, USA

Matthew D. Alexander, MD,
University of California-San Francisco, Department of Radiology, San Francisco, CA

David L. Tirschwell, MD, MSc,
University of Washington, Department of Neurology, Seattle, WA, USA

T. Hatsukami, MD,
University of Washington, Department of Surgery, Seattle, WA, USA

Catherine Amlie-Lefond, MD, and
University of Washington, Department of Neurology, Seattle, WA, USA

C. Yuan, PhD
University of Washington, Department of Radiology, Seattle, WA, USA

Abstract

(corresponding author) Phone: 206-598-3845, Fax: 206-598-8475, mmossab@uw.edu.

Disclosures

Mossa-Basha, de Havenon, Becker, Hallam, Levitt, Tirschwell, Cohen, Alexander, Amlie-Lefond: None Hippe: GE and Philips Healthcare grants unrelated to the current work.

Hatsukami: Philips Healthcare grants unrelated to the current work.

Yuan: Philips Healthcare grants unrelated to the current work. Member of Philips Radiology Medical Advisory Network.

Background and Purpose—Although studies have evaluated the differential imaging of moyamoya disease and atherosclerosis, none have investigated the added value of vessel-wall MRI. The current study evaluates the added diagnostic value of vessel-wall MRI in differentiating moyamoya disease (MMD), atherosclerotic-moyamoya syndrome (A-MMS) and vasculitic-moyamoya syndrome (V-MMS) with a multi-contrast protocol.

Methods—We retrospectively reviewed the carotid artery territories of patients with clinically defined vasculopathies (MMD, atherosclerosis, vasculitis) and steno-occlusive intracranial carotid disease. Two neuroradiologists, blinded to clinical data reviewed the luminal imaging of each carotid, evaluating collateral extent and making a presumed diagnosis with diagnostic confidence. After three weeks, the two readers reviewed the luminal imaging+vessel-wall MRI for presence, pattern and intensity of post-contrast enhancement, T2 signal characteristics, pattern of involvement, presumed diagnosis and confidence.

Results—Ten A-MMS, three V-MMS and eight MMD cases with 38 affected carotid segments were included. There was significant improvement in diagnostic accuracy with luminal imaging +vessel-wall MRI as compared to luminal imaging (87% vs. 32%, p<.001). The most common vessel-wall MRI findings for MMD were non-enhancing, non-remodeling lesions without T2 heterogeneity; for A-MMS eccentric, remodeling, and T2 heterogeneous lesions with mild/moderate and homogeneous/heterogeneous enhancement; and for V-MMS concentric lesions with homogeneous, moderate enhancement. Inter-reader agreement was moderate to substantial for all vessel-wall MRI characteristics (κ=0.46-0.86) and fair for collateral grading (κ=0.35). There was 11% inter-reader agreement for diagnosis on luminal imaging as compared to 82% for luminal imaging+vessel-wall MRI (p<.001).

Conclusion—Vessel-wall MRI can significantly improve the differentiation of moyamoya vasculopathies when combined with traditional imaging techniques.

Keywords

Magnetic Resonance Imaging; Differentiation; Moyamoya disease; Moyamoya; Vessel Wall Imaging

Introduction

Moyamoya vasculopathy which is divided into moyamoya disease (MMD) and moyamoya syndrome (MMS), is a steno-occlusive process of the carotid termini, proximal MCA and ACA with development of robust compensatory collaterals at the base of the brain. MMS may arise secondary to a number of underlying disease processes including sickle cell anemia, neurofibromatosis 1, radiation therapy, congenital syndromes, intracranial atherosclerotic disease (A-MMS) and vasculitis (V-MMS). It is important to differentiate MMD from other causes of MMS, as treatment may differ drastically[,] . Specifically, the first line therapy for symptomatic MMD is surgical revascularization, while the Stenting and Aggressive Medical Management for Preventing Recurrent Stroke in Intracranial Stenosis (SAMMPRIS) trial showed that aggressive medical management is the first line therapy for patient with high-grade (70-99%) atherosclerotic stenosis. Similarly, V-MMS should not be surgically treated, but rather treatment should focus on the underlying inflammatory process.

Diagnostic evaluation typically focuses on luminal imaging and clinical features, however, there is significant overlap in luminal patterns of disease between MMD and MMS. Collaterals are compensatory and similar collateralization can be seen in A-MMS or MMD, and depending on the stage of disease, collaterals may not be seen in MMD. In addition, both MMD and MMS can present with either bilateral or unilateral disease. The clinical presentation may not allow for definitive differentiation especially in adult presentations of moyamoya vasculopathy.

There have only been a few studies that evaluated differences in vessel-wall MRI appearances between atherosclerosis and MMD[-]. The current study is the first to assess the added value of a multi-contrast vessel-wall MRI protocol in addition to luminal imaging for differentiation of MMD, A-MMS and V-MMS.

Materials and Methods

Patient Selection

After Institutional Review Board Approval, consecutive patients who had undergone intracranial arterial wall imaging from May 2013 to November 2015 were included from a prospectively maintained database. A neurointerventionalist (ML) reviewed the cases to determine the pattern of luminal disease, and selected cases with Moyamoya vasculopathy (steno-occlusive disease of the carotid terminus, A1 and M1 segments). Two stroke neurologists (KJB, ADH) reviewed the clinical information and imaging reports of pattern of disease, while blinded to vessel-wall MRI information and clinical diagnosis, and categorized the vasculopathies as vasculitis, atherosclerosis, reversible cerebral vasoconstriction syndrome or MMD. If there was disagreement in the diagnosis, a third stroke neurologist (DLT) arbitrated.

Imaging Protocol

Patients were scanned on a 3T Siemens Trio MR scanner (Siemens Healthcare, Erlangen, Germany). The imaging protocol included high-resolution multi-planar T1 (0.4×0.35 in-plane resolution; slice thickness, 2 mm; repetition time/echo time, 1000/10 ms; time, 36 s per slice) pre and post contrast, T2(in-plane, 0.4×0.4; slices, 1 mm; repetition time/echo time, 3550/72 ms; time, 9.3 s per slice) and 3D SPACE T2-weighted (0.6×0.6 mm in-plane resolution; slice thickness, 0.6 mm; repetition time/echo time, 2400/80 ms; slices, 64; time, 10:20 minutes) sequences. More detailed imaging parameters can be found in a prior publication.

Image Analysis

Two independent raters (DKH, WC), blinded to clinical and vessel-wall MRI data, reviewed consecutive luminal studies performed for the moyamoya vasculopathy subjects. The luminal studies included any digital subtraction catheter angiographic (DSA), CTA or MRA study that had been performed prior to the vessel-wall MRI. Each intracranial internal carotid territory was evaluated independently with a brief written description of luminal disease pattern on the contralateral side to provide an idea of the pattern of global disease. The raters evaluated the presence and site of luminal disease, collateral development on a 3-

point scale (0= no collaterals, 1= moderate collaterals, 2= robust collaterals), presumed diagnosis (MMD, V-MMS or A-MMS) and their confidence of diagnosis on a 4-point Likert-like scale (0=equivocal, 1= 60% confidence, 2= 75% confidence, 3= >90% confidence). Raters were allowed to defer diagnosis when confidence was equivocal. After a three-week washout period, the raters independently reviewed vessel-wall and luminal data together for each internal carotid artery with an expanded written description including both luminal and vessel wall patterns of disease on the contralateral side while blinded to patient clinical data. The raters evaluated the pattern of lesion arterial wall involvement (eccentric, concentric), presence of enhancement (y/n), the degree of enhancement (None= equivalent to normal wall, mild= less than the enhancement of the infundibulum, moderate= ≥ the enhancement of the infundibulum), pattern of enhancement (homogeneous was defined as complete enhancement of the lesion, heterogeneous enhancement was incomplete lesion enhancement, and focal enhancement was defined as a point or short linear region of lesional enhancement), outward remodeling (positive if the outer wall area are qualitatively greater than the proximal normal segment), T2 lesion appearance (heterogeneous, not heterogeneous), presence of juxtaluminal T2 hyperintense band, presumed diagnosis and confidence in the diagnosis (using the same 4-point scale). We used a qualitative assessment for outward remodeling to show that in individual cases, this can be evaluated by the radiologist and that it can be assessed and contribute to clinical differentiation in individual patients.

Statistical Analysis

Continuous and categorical variables were summarized as mean ± standard deviation (SD) and count (percentage), respectively. Diagnostic accuracy was computed as the percentage of cases where the rater's presumed diagnosis matched the final clinical diagnosis. Any cases classified as equivocal by the rater, without a presumed diagnosis, were considered an incorrect diagnosis. Diagnostic accuracy was compared between the luminal imaging only session and the luminal imaging+vessel-wall MRI session using McNemar's test. Inter-rater agreement for each individual luminal imaging and vessel-wall MRI finding was summarized as the percentage of cases where the readers gave the same rating (percent agreement) and unweighted Cohen's kappa. Inter-rater agreement for the presumed diagnosis was summarized as percent agreement, with equivocal cases always being considered a disagreement, even if both raters provided an equivocal diagnosis. Percent agreement was compared between luminal imaging and luminal imaging+vessel-wall MRI sessions using McNemar's test. Individual luminal imaging and vessel-wall MRI findings were compared between A-MMS and MMD groups using the Chi-squared trend test (for collateral grade) or the standard Chi-squared test (all other findings). There were too few vasculitis patients for comparison.

Throughout the analysis, the left and right sides were treated as separate—though not independent—observations, as the raters only viewed and rated one side at a time during the review. For the analysis of diagnostic accuracy and prevalence of individual imaging findings, each rater's assessment was also treated as a separate but not independent observation. This approach of pooling the two raters treats them evenly and results correspond to an average of the two. This is a more efficient use of data than analyzing only

one rater or each rater separately. To avoid double counting all cases and treating all observations as independent, all hypothesis tests (McNemar's and Chi-squared tests) were conducted as permutation tests, where all observations from the same patient were permuted together. Clustering all observations from the same patient like this accounts for the dependence between these observations and does not inappropriately inflate the effective sample size. 95% confidence intervals (CIs) for Cohen's kappa were computed using the non-parametric bootstrap with the percentile method, also resampling by patient. All statistical calculations were conducted with the statistical computing language R (version 3.1.1; R Foundation for Statistical Computing, Vienna, Austria). Throughout, two-tailed tests were used with statistical significance defined as $p<0.05$.

Results

Clinical Diagnoses and Characteristics

148 consecutive vessel-wall MRI cases with luminal imaging were reviewed, with 21 found to have moyamoya vasculopathy on luminal imaging. Of these, 10 had A-MMS, 8 had MMD and 3 had V-MMS (all of which were varicella vasculitis). Patient clinical and demographic information are summarized in Table 1. Of note, all A-MMS patients and none of the MMD or V-MMS patients had ≥2 vascular risk factors. Of the 42 hemispheres imaged with luminal imaging, a total of 38 pathological carotid arterial territories were evaluated (2 per patient, with 4 segments determined to be normal on luminal imaging) by 2 independent readers for a total of 76 ratings. Luminal imaging exams performed within each disease group are also listed in Table 1. All cases underwent clinical evaluation based on current diagnostic guidelines. All cases that lacked DSA either fulfilled proposed criteria that obviated the need for DSA, or had clinical diagnoses that ruled out a diagnosis of MMD.

Vessel-Wall MRI Characteristics

There were significant differences in the vessel-wall MRI appearances of A-MMS, V-MMS and MMD (Table 2). Typical findings are shown in Figure 1. A-MMS most frequently had eccentric, outward remodeling lesions that were heterogeneous on T2W vessel-wall MRI and had a juxtaluminal hyperintense band. All A-MMS lesions showed a mild or moderate degree of enhancement that was homogeneous or heterogeneous. In comparison, MMD showed non-eccentric, non-remodeled lesions, without T2 wall signal heterogeneity or a juxtaluminal T2 hyperintense band and rarely enhanced. When enhancement was present with MMD, the lesions were concentric and showed homogeneous, mild enhancement. V-MMS showed concentric moderately enhancing lesions without outward remodeling or T2 lesion heterogeneity.

Added Value of Vessel-Wall MRI

Based on luminal imaging alone, readers made the correct diagnosis (of A-MMS, MMD or V-MMS) in 24 of 76 evaluations (32%). When luminal imaging and vessel-wall MRI were both available, readers were significantly more accurate with 66 of 76 (87%) correctly diagnosed ($p<0.001$) (Table 3). The improvement in diagnostic accuracy was similar for each rater individually (rater 1: 29% to 89%, $p<0.001$; rater 2: 34% to 84%, $p<0.001$). Improvement in diagnostic accuracy with the addition of vessel-wall MRI was seen in A-

MMS (32% vs. 82%, p=0.009), MMD (37% vs. 90%, p=0.016) and V-MMS (13% vs. 100%, p=0.25), though there were only three vasculitis patients (8 readings). Of the 52 readings with an incorrect diagnosis based on luminal imaging alone, 43 (83%) were correctly reclassified with the addition of vessel-wall MRI. One reading correctly diagnosed by luminal imaging as MMD was then incorrectly reclassified by luminal imaging+vessel-wall MRI as A-MMS. There were 9 readings with an incorrect diagnosis by both luminal imaging and luminal imaging+vessel-wall MRI, of which 7 had a clinical diagnosis of A-MMS (misdiagnosed as MMD or equivocal) and 2 MMD (misdiagnosed as A-MMS or equivocal).

Diagnostic Confidence

Readers' confidence rating was the same (4 of 76 or 5.3%) or higher (94.7%) in all cases of the luminal imaging+vessel-wall MRI review compared to the corresponding luminal imaging alone review. On the Likert scale, the average increase in confidence was 2.4 when vessel-wall MRI+luminal imaging correctly reclassified a case, 1.3 when a case was diagnosed correctly by both luminal imaging alone and luminal imaging+vessel-wall MRI, and 1.6 when a case was incorrectly diagnosed by both luminal imaigng alone and luminal imaging+vessel-wall MRI.

Inter-reader Agreement

Inter-reader agreement on the luminal imaging and vessel-wall MRI findings is summarized in Table 4. Agreement was moderate or substantial for most findings, with collateral grade having fair agreement (58% of cases, Cohen's $\kappa = 0.35$). Inter-reader agreement on diagnosis was 11% (4 of 38) based on luminal imaging (all uncertain diagnoses were counted as disagreements) and 82% (31 of 38) using luminal imaging+vessel-wall MRI ($p<0.001$).

Discussion

We report the first study utilizing a multi-contrast vessel-wall MRI protocol for the differentiation of MMD from A-MMS and V-MMS. In addition, this is the first study to assess the added value of vessel-wall MRI over luminal imaging alone in moyamoya vasculopathy differentiation. This study shows that a multi-contrast vessel-wall MRI protocol with luminal imaging can differentiate between MMD and MMS due to atherosclerosis or vasculitis significantly better than luminal imaging alone. We found there was moderate to substantial agreement in all vessel-wall MRI characteristics studied, indicating that vessel-wall MRI characteristics can be consistently evaluated in moyamoya vasculopathy. There was only fair agreement in the assessment of luminal imaging of collaterals. The likelihood of a correct diagnosis in the setting of moyamoya vasculopathy significantly increased when vessel-wall MRI was combined with luminal imaging (from 31.6% to 86.8%, p<.001), and this increase was significant for MMD and A-MMS. While the increase in diagnostic accuracy was not statistically significant for vasculitis, given the study was underpowered to detect such a difference, the accuracy increased from 12.5% to 100% with the inclusion of vessel-wall MRI. In addition, rater confidence increased with direct visualization of vessel wall abnormalities.

Historically, angiographic imaging has served as the reference standard for differentiation of MMD from A-MMS, with differentiating features considered to be prominent moyamoya collaterals and bilaterality of carotid terminus steno-occlusive disease. However, limiting the diagnostic accuracy of luminal imaging are the observations that collaterals are compensatory, frequently visualized in A-MMS[9] , only present in the intermediate stages of MMD evolution, and both MMD and MMS can be unilateral or bilateral. In the current study, we found distinctive patterns of vessel-wall MRI appearance in MMD, AMMS and V-MMS that improve diagnostic accuracy over angiography and other forms of luminal imaging alone. MMD most commonly showed no post-contrast vessel wall enhancement and absence of eccentric wall thickening, no outward remodeling, lack of heterogeneous T2 wall signal and absent juxtaluminal T2 hyperintense band. When wall enhancement was seen in MMD (13%), it was mild, concentric, homogeneous enhancement which differed in appearance from both A-MMS and V-MMS. A-MMS showed eccentric and outwardly remodeling wall thickening with heterogeneous lesion T2 signal, a juxtaluminal T2 hyperintense band and heterogeneous or homogeneous, mild or moderate lesion enhancement. V-MMS showed concentric, moderate, homogeneously enhancing lesions without T2 lesion heterogeneity, juxtaluminal T2 hyperintense band nor outward remodeling.

There have been a few studies that have compared MMD to atherosclerosis on vessel-wall MRI. Kim et al compared 12 MMD and 20 atherosclerosis patients using vessel-wall MRI, and found that MMD typically showed non-eccentric, non-enhancing lesions with wall shrinkage, while atherosclerosis showed eccentric, enhancing and outward remodeling lesions. Yuan et al compared 21 MMD and 44 atherosclerosis subjects, and found that on vessel-wall MRI, MMD typically shows concentric wall thickening with homogeneous signal as compared to eccentric, heterogeneous atherosclerotic lesions. These studies agree with our findings that atherosclerotic lesions show outward remodeling and heterogeneous wall signal, but in addition, we showed atherosclerosis differs from MMD by having a T2 hyperintense juxtaluminal band and either homogeneous or heterogeneous lesion enhancement, while MMD typically does not show appreciable wall thickening and rarely enhances. Ryoo et al assessed 25 MMD, 7 probable MMD and 16 atherosclerosis patients on vessel-wall MRI, and found that 90.6% of MMD and probable MMD typically showed circumferential wall enhancement at the carotid termini with wall shrinkage, while atherosclerotic lesions typically showed eccentric wall enhancement and outward remodeling. This study's findings differ from the above-mentioned studies and our own in regards to the frequency of wall enhancement in MMD. In our study, we found that 13% of MMD lesions show mild, circumferential enhancement, which is a substantially lower rate. This discrepancy may be due to the heterogeneity of the genetic background of MMD[9] and that this study may have captured a subtype of MMD with differences in pathophysiology. Ryoo et al evaluated Korean patients with MMD, while our MMD population was either Caucasian or Hispanic; the two populations have different genetic susceptibility with different biochemical pathways. Another possibility is that MMD or subtypes of MMD are transiently inflammatory, and Ryoo et al's study captured these patients during this intermediate stage.

There are several limitations to this work. First, this was a retrospective study. Second, the luminal imaging modalities performed were heterogeneous, however, best practice guidelines were utilized for imaging performance and patient care, and the approach to image review best approximates clinical practice at many institutions. Third, the sample size is limited as moyamoya vasculopathy is uncommon, especially MMD and V-MMS. Fourth, there is no histology confirmation of diagnosis, and in the setting of MMD and A-MMS, the only gold standard is autopsy evaluation, which was not used in the current study. We rather relied on the expert review of 3 stroke neurologists, who had access to the comprehensive diagnostic workups, as a reference standard. Further multi-center investigation with inclusion of genotypic and phenotypic analysis would be helpful to better classify the imaging appearances of MMD, better define its subtypes, and illuminate disease pathophysiology and progression.

Conclusion

Vessel-wall MRI improves diagnostic accuracy and diagnostic confidence in the differentiation of moyamoya disease from atherosclerotic and vasculitic moyamoya syndrome compared to luminal imaging alone. The differentiation is important as treatments for each disease entity differ significantly. Care needs to be taken when making conclusions based on a limited number of cases and this study requires replication in a larger independent cohort. However, if further confirmed in larger studies, the diagnostic algorithm and criteria for moyamoya disease may be revised for improved diagnostic accuracy in addition to potentially limiting invasive diagnostic tests.

Acknowledgments

Funding Sources

The study was supported by the NIH 1R56NS092207-01 grant fund from the National Institute of Neurodegenerative Disorders and Stroke.

References

1. Scott RM, Smith ER. Moyamoya disease and moyamoya syndrome. The New England journal of medicine. 2009; 360:1226–1237. [PubMed: 19297575]
2. Derdeyn CP, Chimowitz MI, Lynn MJ, Fiorella D, Turan TN, Janis LS, et al. Aggressive medical treatment with or without stenting in high-risk patients with intracranial artery stenosis (sammpris): The final results of a randomised trial. Lancet (London, England). 2014; 383:333–341.
3. Research Committee on the Pathology Treatment of Spontaneous Occlusion of the Circle of Willis: Health Labour Sciences Research Grant for Research on Measures for Infractable Diseases. Guidelines for diagnosis and treatment of moyamoya disease (spontaneous occlusion of the circle of willis). Neurologia medico-chirurgica. 2012; 52:245–266. [PubMed: 22870528]
4. Togao O, Mihara F, Yoshiura T, Tanaka A, Noguchi T, Kuwabara Y, et al. Cerebral hemodynamics in moyamoya disease: Correlation between perfusion-weighted mr imaging and cerebral angiography. AJNR. American journal of neuroradiology. 2006; 27:391–397. [PubMed: 16484417]
5. Tanaka M, Sakaguchi M, Kitagawa K. Mechanism of moyamoya vessels secondary to intracranial atherosclerotic disease: Angiographic findings in patients with middle cerebral artery occlusion. Journal of stroke and cerebrovascular diseases : the official journal of National Stroke Association. 2012; 21:373–378. [PubMed: 21111634]

6. Wei YC, Liu CH, Chang TY, Chin SC, Chang CH, Huang KL, et al. Coexisting diseases of moyamoya vasculopathy. Journal of stroke and cerebrovascular diseases : the official journal of National Stroke Association. 2014; 23:1344–1350. [PubMed: 24468071]
7. Suzuki J, Takaku A. Cerebrovascular “moyamoya” disease. Disease showing abnormal net-like vessels in base of brain. Archives of neurology. 1969; 20:288–299. [PubMed: 5775283]
8. Kim YJ, Lee DH, Kwon JY, Kang DW, Suh DC, Kim JS, et al. High resolution mri difference between moyamoya disease and intracranial atherosclerosis. European journal of neurology. 2013; 20:1311–1318. [PubMed: 23789981]
9. Ryoo S, Cha J, Kim SJ, Choi JW, Ki CS, Kim KH, et al. High-resolution magnetic resonance wall imaging findings of moyamoya disease. Stroke; a journal of cerebral circulation. 2014; 45:2457–2460.
10. Yuan M, Liu ZQ, Wang ZQ, Li B, Xu LJ, Xiao XL. High-resolution MR imaging of the arterial wall in moyamoya disease. Neurosci Lett. 2015 Jan 1.584:77–82. [PubMed: 25459282]
11. Mossa-Basha M, Hwang WD, De Havenon A, Hippe D, Balu N, Becker KJ, et al. Multicontrast high-resolution vessel wall magnetic resonance imaging and its value in differentiating intracranial vasculopathic processes. Stroke; a journal of cerebral circulation. 2015; 46:1567–1573.
12. Qiao Y, Zeiler SR, Mirbagheri S, Leigh R, Urrutia V, Wityk R, et al. Intracranial plaque enhancement in patients with cerebrovascular events on high-spatial-resolution mr images. Radiology. 2014; 271:534–542. [PubMed: 24475850]
13. A.C. Davison, DVH. Bootstrap methods and their application. Cambridge University Press; Cambridge, United Kingdom: 1997.
14. Liu W, Morito D, Takashima S, Mineharu Y, Kobayashi H, Hitomi T, et al. Identification of rnf213 as a susceptibility gene for moyamoya disease and its possible role in vascular development. PloS one. 2011; 6:e22542. [PubMed: 21799892]
15. Milewicz DM, Kwartler CS, Papke CL, Regalado ES, Cao J, Reid AJ. Genetic variants promoting smooth muscle cell proliferation can result in diffuse and diverse vascular diseases: Evidence for a hyperplastic vasculomyopathy. Genetics in medicine : official journal of the American College of Medical Genetics. 2010; 12:196–203. [PubMed: 20130469]
16. Shoemaker LD, Clark MJ, Patwardhan A, Chandratillake G, Garcia S, Chen R, et al. Disease variant landscape of a large multiethnic population of moyamoya patients by exome sequencing. G3 (Bethesda, Md.). 2015; 6:41–49.
17. Masuda J, Ogata J, Yutani C. Smooth muscle cell proliferation and localization of macrophages and t cells in the occlusive intracranial major arteries in moyamoya disease. Stroke; a journal of cerebral circulation. 1993; 24:1960–1967.

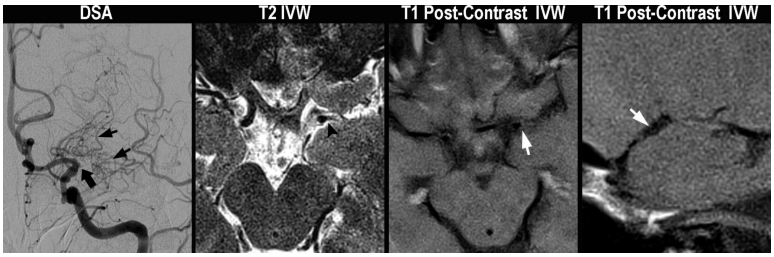

Figure 0001

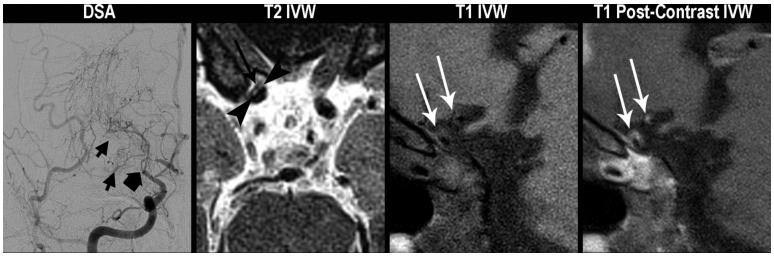

Figure 0002

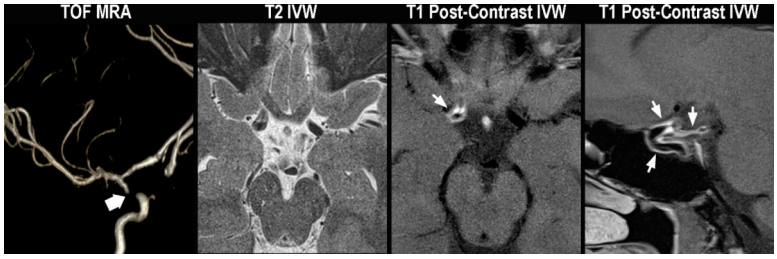

Figure 0003

Figure 1.

Typical patterns of moyamoya vasculopathies. **Moyamoya disease (A)**. A 43 year-old female without vascular risk factors presents with a left MCA territory stroke. On DSA, left common carotid injection (left image), there is irregularity of the left carotid terminus and occlusion of the MCA origin (thick black arrow) with formation of collaterals (short black arrows). On axial T2 vessel-wall MRI (middle left image), there is no significant wall thickening or outward remodeling proximal to or at the level of occlusion (black arrowhead). On axial (middle right image) and sagittal (right image) T1 post-contrast images, there is no evidence of appreciable wall thickening, abnormal wall enhancement, lesion eccentricity, or outward remodeling just proximal to occlusion (short white arrow). **A-MMS (B).** A 45 year-old female with history of prior strokes, hypertension, hyperlipidemia, type II diabetes mellitus, and BMI of 33 presents with a right MCA stroke. On DSA, right internal carotid injection (left image), there is occlusion of the right carotid terminus (thick black arrow) with formation of collaterals (short black arrows). Axial T2 vessel-wall MRI (middle left image) demonstrates eccentric wall thickening with lesion heterogeneity and juxtaluminal T2 hyperintensity (black arrowheads) that has lower signal intensity than CSF representing fibrous cap, as well as superficial hypointensity (long black arrow) representing lipid rich necrotic core. On sagittal T1 pre- (middle right image) and post-contrast (right image) vessel-wall MRI images, there are eccentric, outward remodeling, enhancing lesions

involving the carotid terminus and A1 ACA (white arrows). **V-MMS (C).** A 25 year-old female presents after a syncopal episode with right MCA stroke who was found to have CSF evidence of active VZV infection. On 3D maximum intensity projection reformatted image of the right internal carotid artery territory (left image), there is high-grade stenosis of the right carotid terminus (thick white arrow). Axial T2 vessel-wall MRI (middle left image) shows circumferential wall thickening. Axial (middle right image) and sagittal (right image) T1 post-contrast vessel-wall MRI shows circumferential, homogeneous, moderate vessel wall enhancement involving the right intracranial internal carotid artery and posterior communicating artery (short white arrows).

Table 1

Clinical characteristics.

			Final Diagnosis		
Variable		**All (N=21)**	**ICAD (N=10)**	**MMD (N=8)**	**V (N=3)**
Age – years		41 ± 14	49 ± 14	35 ± 11	30 ± 3
Gender	Male	3 (14.3)	1 (10.0)	2 (25.0)	0 (0.0)
	Female	18 (85.7)	9 (90.0)	6 (75.0)	3 (100.0)
Race	Caucasian	10 (47.6)	4 (40.0)	5 (62.5)	1 (33.3)
	Asian	1 (4.8)	1 (10.0)	0 (0.0)	0 (0.0)
	Hispanic	9 (42.9)	4 (40.0)	3 (37.5)	2 (66.7)
	Black	1 (4.8)	1 (10.0)	0 (0.0)	0 (0.0)
Risk factors	Hypertension	8 (38.1)	8 (80.0)	0 (0.0)	0 (0.0)
	Hyperlipidemia	9 (42.9)	8 (80.0)	1 (12.5)	0 (0.0)
	Diabetes	7 (33.3)	6 (60.0)	1 (12.5)	0 (0.0)
	Obesity*	8 (38.1)	6 (60.0)	2 (25.0)	0 (0.0)
	Current smoker	1 (4.8)	1 (10.0)	0 (0.0)	0 (0.0)
	Coronary artery disease	0 (0.0)	0 (0.0)	0 (0.0)	0 (0.0)
No. of risk factors	0	7 (33.3)	0 (0.0)	4 (50.0)	3 (100.0)
	1	4 (19.1)	0 (0.0)	4 (50.0)	0 (0.0)
	2-4	10 (47.6)	10 (100.0)	0 (0.0)	0 (0.0)
Luminal Imaging	DSA	13 (61.9)	5 (50.0)	8 (100.0)	0 (0.0)
	CTA	15 (71.4)	8 (80.0)	6 (75.0)	1 (33.3)
	MRA	21 (100.0)	10 (100.0)	8 (100.0)	3 (100.0)

Values are mean ± SD or no. (%);

ICAD = intracranial atherosclerotic disease; MMD = moyamoya disease; V = vasculitis;

*Body mass index > 30 kg/m^2.

Table 2

Luminal imaging and vessel-wall MRI findings for each disease group (N=76 arterial territories; left and right sides, two readers each).

		Final Diagnosis			
Luminal Findings		**ICAD (N=38)**	**MMD (N=30)**	**V (N=8)**	**P-value (ICAD vs. MMD)** *
Occlusion	ACA	0 (0.0)	2 (6.7)	0 (0.0)	0.95 †
	MCA	11 (28.9)	6 (20.0)	1 (12.5)	
	ICA	14 (36.8)	12 (40.0)	2 (25.0)	
	SCA	1 (2.6)	0 (0.0)	0 (0.0)	
	None	13 (34.2)	10 (33.3)	5 (62.5)	
Collaterals	None	19 (50.0)	6 (20.0)	8 (100.0)	**0.033**
	Some	15 (39.5)	13 (43.3)	0 (0.0)	
	Pronounced	4 (10.5)	11 (36.7)	0 (0.0)	
VMI Findings					
Eccentric lesion		24 (63.2)	3 (10.0)	0 (0.0)	**0.010**
Remodeling	Outward	22 (57.9)	2 (6.7)	0 (0.0)	**0.003**
T2 signal of VW	Heterogenous	21 (55.3)	0 (0.0)	3 (37.5)	**0.006**
	Juxtaluminal hyperintensity	20 (52.6)	0 (0.0)	0 (0.0)	
VW enhancement	Yes	25 (65.8)	4 (13.3)	8 (100.0)	**0.010**
Enhancement intensity	Mild	16 (64.0)	4 (100.0)	0 (0.0)	0.30
(if enhanced)	Moderate	9 (36.0)	0 (0.0)	8 (100.0)	
Pattern of enhancement	Focal	2 (8.0)	0 (0.0)	0 (0.0)	0.41
(if enhanced)	Homogeneous	11 (44.0)	4 (100.0)	6 (75.0)	
	Heterogeneous	12 (48.0)	0 (0.0)	2 (25.0)	

Values are no. (%) unless otherwise specified;

ACA = anterior cerebral artery; ICA = internal carotid artery; ICAD = intracranial atherosclerotic disease; LI = luminal imaging; MCA = middle cerebral artery; MMD = moyamoya disease; SCA = superior cerebellar artery; V = vasculitis; IVWM = vessel wall imaging;

*Permutation-test based on the standard Chi-squared test statistic or trend statistic (collateral grade only); only ICAD and MMD groups were compared because the vasculitis group had only three patients;

†Comparison of any occlusion vs. no occlusion.

Table 3

Change in diagnostic accuracy (% with correct diagnosis) from luminal imaging to luminal + vessel-wall MRI.

		Imaging Modality		
Group*	**No.**	**LI**	**LI+IVWM**	**P-value†**
All	76	24 (31.6)	66 (86.8)	**<0.001**
ICAD	38	12 (31.6)	31 (81.6)	**0.009**
MMD	30	11 (36.7)	27 (90.0)	**0.016**
V	8	1 (12.5)	8 (100.0)	0.25

ICAD = intracranial atherosclerotic disease; LI = luminal imaging; MMD = moyamoya disease; V = vasculitis; IVWM = vessel wall imaging;

*Group defined as either all cases or based on the final clinical diagnosis;

†Permutation test based on McNemar's test statistic.

Table 4

Inter-reader agreement of luminal imaging and vessel-wall MRI findings (N=38).

		Reader		Agreement		
Luminal Findings		**R1**	**R2**	**% Agree**	**Cohen's K**	**(95% CI)**
Collaterals	None	14 (36.8)	19 (50.0)	57.9	0.35	(0.07-0.61)
	Mild	15 (39.5)	13 (34.2)			
	Robust	9 (23.7)	6 (15.8)			
IVWM Findings						
Eccentric lesion		13 (34.2)	14 (36.8)	81.6	0.60	(0.30-0.85)
Remodeling	Outward	12 (31.6)	12 (31.6)	84.2	0.63	(0.40-0.85)
T2 signal of vessel wall	Heterogenous	12 (31.6)	12 (31.6)	89.5	0.76	(0.51-0.94)
	Juxtaluminal hyperintensity	11 (28.9)	9 (23.7)	94.7	0.86	(0.64-1.00)
Vessel wall enhancement	Yes	18 (47.4)	19 (50.0)	92.1	0.84	(0.65-1.00)
Enhancement intensity* (if enhanced)	Mild	6 (35.3)	11 (64.7)	70.6	0.46	(0.10-1.00)
	Moderate	11 (64.7)	6 (35.3)			
Pattern of enhancement* (if enhanced)	Focal	1 (5.9)	1 (5.9)	82.4	0.68	(0.23-1.00)
	Homogeneous	11 (64.7)	8 (47.1)			
	Heterogeneous	5 (29.4)	8 (47.1)			

Values are no. (%) unless otherwise specified;

ACA = anterior cerebral artery; MCA = middle cerebral artery; ICA = internal carotid artery; SCA = superior cerebellar artery;

*Based on the 17 cases where both readers agreed on the presence of enhancement.